Semiclassical calculations of the anisotropic magnetoresistance of NiFe-based thin films, wires, and multilayers

Th. G. S. M. Rijks
Department of Physics, Eindhoven University of Technology, P.O. Box 513, 5600 MB Eindhoven, The Netherlands and Philips Research Laboratories, Prof. Holstlaan 4, 5656 AA Eindhoven, The Netherlands

R. Coehoorn
Philips Research Laboratories, Prof. Holstlaan 4, 5656 AA Eindhoven, The Netherlands

M. J. M. de Jong
Philips Research Laboratories, Prof. Holstlaan 4, 5656 AA Eindhoven, The Netherlands and Instituut-Lorentz, University of Leiden, 2300 RA Leiden, The Netherlands

W. J. M. de Jonge
Department of Physics, Eindhoven University of Technology, P.O. Box 513, 5600 MB Eindhoven, The Netherlands
(Received 26 August 1994)

The anisotropic magnetoresistance (AMR) at low temperatures is theoretically studied for low-dimensional NiFe-based systems in various geometries by solving the Boltzmann transport equation. The AMR is treated by introducing spin-dependent anisotropic mean free paths, making use of anisotropic-scattering parameters that are extracted from experimental spin-resolved resistivity data for bulk dilute NiFe alloys. A first set of calculations comprises the AMR in NiFe thin films and cylindrical wires, as a function of the layer thickness and wire diameter, respectively. For the thin film case we have considered rotation of the magnetization vector within the film plane as well as out of the film plane. For the latter the highest AMR ratio is found, which even slightly exceeds the bulk value. For wires the dependence of the AMR on the dimensions is qualitatively different as compared to the film case due to the relatively enhanced importance of boundary scattering. Finally, the validity of a description of the combined effect of AMR and the giant magnetoresistance in terms of a simple summation of the two effects is studied by performing model calculations for NiFe/Cu/NiFe trilayers.

I. INTRODUCTION

In 1857 Thomson discovered that the resistivity of a ferromagnetic metal may depend on the angle between the current and magnetization direction.[1] A century later the first systematic investigations on the origin of this so-called anisotropic magnetoresistance effect (AMR) were carried out. Theoretical investigations, by Smit,[2] Berger,[3] and Potter,[4] showed that the effect arises from anisotropic scattering due to spin-orbit interaction. Experimental work was carried out by Smit,[2] van Elst,[5] McGuire and Potter,[6] Dorleijn and co-workers,[7,8] and Jaoul, Campbell, and Fert.[9] It was found that a number of alloys, based on iron, cobalt, or nickel, exhibit a rather large AMR effect, which proves to be of technical interest in the field of magnetic recording.[10,11]

A measure for the size of this effect is the AMR ratio, defined as $(\rho_{\parallel}-\rho_{\perp})/\rho_{\parallel}$, in which $\rho_{\parallel}$ and $\rho_{\perp}$ are the resistivities with the magnetization parallel and perpendicular to the current direction, respectively. Whereas for transition-metal alloys the largest effect is found for $Ni_{70}Co_{30}$, viz., 26.7% at 4.2 K and 6.6% at room temperature,[6] alloys with compositions close to $Ni_{80}Fe_{20}$ (permalloy) have been found to be most suitable for sensor applications because of their high permeability and low magnetostriction. Thin permalloy films (thickness 300–500 Å) show an AMR ratio of about 2% at room temperature. This value is much smaller than the AMR ratio in bulk samples, which amounts to 4% at room temperature. There are two effects that may contribute to this difference. First, the thin films studied may be structurally less well defined than bulk specimen, leading to additional electron scattering at grain boundaries and other defects.[12] Second, diffusive scattering at the outer boundaries of the film may affect the AMR ratio. The latter dimensionality effect will be the subject of this paper.

Our approach is basically very similar to the Fuchs-Sondheimer theory[13,14] for the resistivity of nonferromagnetic thin films, which involves the solution of the Boltzmann transport equation in linear response for a free electron gas in the relaxation-time approximation, with the assumption of diffusive scattering at the outer boundaries of the film. Our crucial additional assumptions are that (i) the resistivity of a ferromagnetic alloy (near $T=0$ K) is well described by the two-current model, within which the total current is given by independent contributions from majority spin and minority spin electrons (no spin-flip scattering), and that (ii) the mean free path of an electron depends on its spin and, in order to treat the AMR effect, on the angle between its velocity

vector $\mathbf{v}$ and the magnetization vector $\mathbf{M}$. The two-current model has been proposed by Mott[15] and its validity is supported strongly by experimental evidence, e.g., from studies of dilute binary and ternary alloy systems.[7,8] Our second assumption has been put forward earlier by Smit,[2] Berger,[3] and Potter.[4] Here we will not discuss the microscopic origin of the spin and angular dependence of the electron mean free path. Instead we make use of a parametrization scheme which consistently describes the AMR effect of bulk alloys, and the separate contributions from majority and minority spin electrons. To be specific, our numerical examples have been given for dilute NiFe alloys. However, our method can be applied more generally to other alloys for which sufficient experimental information on the AMR effect is available.[7,8]

The model enables us to predict the magnetoresistance effects for various geometries. In Sec. II we present the general model, the application to bulk ferromagnetic alloy systems and to single layers, cylindrical wires and trilayers of the type *F/NM/F*, where *F* and *NM* are ferromagnetic and nonmagnetic layers, respectively. Such trilayers show, in addition to the AMR effect, the giant magnetoresistance effect (GMR): the resistivity decreases upon the orientation of the magnetization directions of the *F* layers from antiparallel to parallel.[16,17] Our method allows a complete calculation of the resistance as a function of both magnetization directions. One of the important questions then is to what extent the AMR and GMR effects can simply be superimposed, in order to obtain the total magnetoresistance effect. We have already briefly addressed this question in an earlier paper,[18] and we will more extensively discuss this topic here. In Sec. III numerical results for NiFe-based systems are presented and discussed. Section IV contains the conclusions.

II. THEORETICAL DESCRIPTION

A. General model

The electrons involved in transport are regarded as a free-electron gas with a spherical Fermi surface. Our model calculations of the resistivity are based on the Boltzmann transport equation in linear response: the electron distribution function, at position $\mathbf{r}$ and with velocity $\mathbf{v}$, is written in the form

$$f^{\uparrow(\downarrow)}(\mathbf{v},\mathbf{r})=f_0^{\uparrow(\downarrow)}(\varepsilon)+g^{\uparrow(\downarrow)}(\mathbf{v},\mathbf{r}) . \tag{1}$$

Here $f_0^{\uparrow(\downarrow)}(\varepsilon)$ is the Fermi-Dirac equilibrium distribution at energy $\varepsilon=\frac{1}{2}mv^2$ and $g^{\uparrow(\downarrow)}(\mathbf{v},\mathbf{r})$ is the deviation from equilibrium in the presence of an electric field $\mathbf{E}$, for majority ($\uparrow$) and minority ($\downarrow$) spin electrons. The linear response Boltzmann transport equation in the relaxation-time approximation is given by

$$\mathbf{v}\cdot\frac{\partial g^{\uparrow(\downarrow)}(\mathbf{v},\mathbf{r})}{\partial \mathbf{r}}-e\mathbf{E}\cdot\mathbf{v}\frac{\partial f_0^{\uparrow(\downarrow)}(\varepsilon)}{\partial\varepsilon}=-\frac{g^{\uparrow(\downarrow)}(\mathbf{v},\mathbf{r})}{\tau^{\uparrow(\downarrow)}} , \tag{2}$$

in which e and m are the electronic charge and mass, respectively, and $\tau^{\uparrow(\downarrow)}$ is the spin-dependent relaxation time. At low temperatures only electrons at the Fermi energy are to be considered. We therefore write $\tau^{\uparrow(\downarrow)}=\lambda^{\uparrow(\downarrow)}/v_F$, in which $\lambda^{\uparrow(\downarrow)}$ is the electron mean free path. The Fermi velocity v_F is assumed to be equal for both spins. The current density for majority and minority spins follows from integrating the solution of the Boltzmann equation over the velocity space according to

$$\mathbf{J}^{\uparrow(\downarrow)}(\mathbf{r})=-e\left[\frac{m}{h}\right]^3\int d^3v\,\mathbf{v}g^{\uparrow(\downarrow)}(\mathbf{v},\mathbf{r}) , \tag{3}$$

in which h is Planck's constant.

In order to treat the AMR, we assume a dependence of the mean free path on the angle ϑ between the electron velocity $\mathbf{v}$ and the magnetization $\mathbf{M}$. This intrinsically anisotropic mean free path for majority and minority spin electrons is given by

$$\lambda^{\uparrow(\downarrow)}(\vartheta)=\lambda_0^{\uparrow(\downarrow)}(1-a^{\uparrow(\downarrow)}\cos^2\vartheta-b^{\uparrow(\downarrow)}\cos^4\vartheta) . \tag{4}$$

The parameters $a^{\uparrow(\downarrow)}$ and $b^{\uparrow(\downarrow)}$ are a measure for the anisotropy of the scattering. Higher-order terms are neglected, as suggested by a microscopic treatment of the AMR effect based on *sd* scattering.[4] Note that in our model, apart from the spin- and angular-dependent mean free path [Eq. (4)], electrons of both spins have identical properties such as mass, Fermi velocity, and density of states. The model can easily be extended to a more realistic electronic structure, and this might be necessary to obtain quantitative agreement with future experiments. However, we feel that our simple model already contains the key ingredients to describe at least qualitatively the size effects, related to the system dimensions, in the conductance of low-dimensional systems and might give directions for novel experiments.

B. Bulk materials

For bulk materials the nonequilibrium distribution g is independent of $\mathbf{r}$. The solution of the Boltzmann equation [Eq. (2)] is then given by

$$g^{\uparrow(\downarrow)}(\hat{\mathbf{v}})=eE\hat{v}_x\left[\frac{\partial f_0(\varepsilon)}{\partial\varepsilon}\right]\lambda^{\uparrow(\downarrow)}(\vartheta) , \tag{5}$$

where $\mathbf{E}$ is directed along the x axis and $\hat{v}_x$ is the x component of unit vector $\hat{\mathbf{v}}\equiv\mathbf{v}/v_F$. Substitution of Eq. (5) into Eq. (3) yields the spin current density $\mathbf{J}^{\uparrow(\downarrow)}$ and thus the conductivity per spin $\sigma^{\uparrow(\downarrow)}$:

$$\sigma^{\uparrow(\downarrow)}\equiv\frac{J^{\uparrow(\downarrow)}}{E}=\frac{ne^2}{2mv_F}\frac{3}{4\pi}\int d^3\hat{v}\hat{v}_x^2\lambda^{\uparrow(\downarrow)}(\vartheta) , \tag{6}$$

where n is the total (majority and minority spin) conduction electron density, given by

$$n=\frac{8\pi}{3}\left[\frac{mv_F}{h}\right]^3 . \tag{7}$$

Evaluation of Eq. (6) yields the well-known Drude result if the mean free path is isotropic. In the case of anisotropic mean free paths, as given by Eq. (4), the conductivity per spin is a function of the angle Θ between $\mathbf{M}$ and $\mathbf{E}$:

$$\sigma^{\uparrow(\downarrow)}(\Theta)=\frac{ne^2}{2mv_F}\lambda_0^{\uparrow(\downarrow)}[1-\tfrac{1}{5}a^{\uparrow(\downarrow)}(1+2\cos^2\Theta) - \tfrac{3}{35}b^{\uparrow(\downarrow)}(1+4\cos^2\Theta)] ,$$

$$=\frac{ne^2}{2mv_F}\lambda_0^{\uparrow(\downarrow)}[1-\tfrac{1}{5}a^{\uparrow(\downarrow)}-\tfrac{3}{35}b^{\uparrow(\downarrow)} -(\tfrac{2}{5}a^{\uparrow(\downarrow)}+\tfrac{12}{35}b^{\uparrow(\downarrow)})\cos^2\Theta] . \quad (8)$$

It thus follows that, even if the microscopic scattering mechanism leads to a mean free path that contains a fourth power term in $\cos\vartheta$, the conductivity only contains the second power $\cos\Theta$ term. The separate contributions of majority and minority spin electrons to the AMR effect are given by

$$\left[\frac{\rho_\parallel-\rho_\perp}{\rho_\parallel}\right]^{\uparrow(\downarrow)}=\left[\frac{\sigma_\perp-\sigma_\parallel}{\sigma_\perp}\right]^{\uparrow(\downarrow)}=\frac{\frac{2}{5}a^{\uparrow(\downarrow)}+\frac{12}{35}b^{\uparrow(\downarrow)}}{1-\frac{1}{5}a^{\uparrow(\downarrow)}-\frac{3}{35}b^{\uparrow(\downarrow)}} . \quad (9)$$

For the total AMR effect we find

$$\left[\frac{\rho_\parallel-\rho_\perp}{\rho_\parallel}\right]=\left[\frac{\sigma_\perp-\sigma_\parallel}{\sigma_\perp}\right] =\frac{\lambda_0^{\uparrow}(\frac{2}{5}a^{\uparrow}+\frac{12}{35}b^{\uparrow})+\lambda_0^{\downarrow}(\frac{2}{5}a^{\downarrow}+\frac{12}{35}b^{\downarrow})}{\lambda_0^{\uparrow}(1-\frac{1}{5}a^{\uparrow}-\frac{3}{35}b^{\uparrow})+\lambda_0^{\downarrow}(1-\frac{1}{5}a^{\downarrow}-\frac{3}{35}b^{\downarrow})} . \quad (10)$$

Information on the parameters $\lambda_0^{\uparrow(\downarrow)}$, $a^{\uparrow(\downarrow)}$, and $b^{\uparrow(\downarrow)}$ can be obtained from the analysis of spin- and angular-resolved resistivity data, as we will show in Sec. III.

C. Thin films

We now study electron transport through a film of thickness t, with outer boundaries at $z=0$ and $z=t$. The electric field $\mathbf{E}$ is directed along the x axis. We assume that the scattering at the outer boundaries of the film is purely diffusive, which implies

$$g^{\uparrow(\downarrow)}(\hat{\mathbf{v}},0)=0, \quad \text{if } \hat{v}_z>0 , \quad (11a)$$

$$g^{\uparrow(\downarrow)}(\hat{\mathbf{v}},t)=0, \quad \text{if } \hat{v}_z<0 . \quad (11b)$$

The solution g of Eq. (2) has now a spatial dependence on the z coordinate, and can be put into the form[13,14,19]

$$g^{\uparrow(\downarrow)}(\hat{\mathbf{v}},z)=eE\hat{v}_x\left[\frac{\partial f_0(\varepsilon)}{\partial\varepsilon}\right]\lambda_{\text{eff}}^{\uparrow(\downarrow)}(\hat{\mathbf{v}},z) . \quad (12)$$

The effective mean free path $\lambda_{\text{eff}}^{\uparrow(\downarrow)}(\hat{\mathbf{v}},z)$ includes bulk scattering as well as scattering at the film boundaries:

$$\lambda_{\text{eff}}^{\uparrow(\downarrow)}(\hat{\mathbf{v}},z)=\lambda^{\uparrow(\downarrow)}(\vartheta)\left[1-\exp\left[\frac{-z}{\lambda^{\uparrow(\downarrow)}(\vartheta)\hat{v}_z}\right]\right], \quad \text{if } v_z>0 , \quad (13a)$$

$$\lambda_{\text{eff}}^{\uparrow(\downarrow)}(\hat{\mathbf{v}},z)=\lambda^{\uparrow(\downarrow)}(\vartheta)\left[1-\exp\left[\frac{t-z}{\lambda^{\uparrow(\downarrow)}(\vartheta)\hat{v}_z}\right]\right], \quad \text{if } v_z<0 . \quad (13b)$$

Note that this form of $\lambda_{\text{eff}}^{\uparrow(\downarrow)}(\hat{\mathbf{v}},z)$, combined with Eq. (12), indeed obeys the boundary conditions of Eq. (11). The conductivity per spin as a function of the angle between $\mathbf{M}$ and $\mathbf{E}$ follows from integrating $g^{\uparrow(\downarrow)}(\hat{\mathbf{v}},z)$, as given by Eq. (12), combined with Eqs. (4) and (13) over a unit sphere in velocity space, using Eq. (3), and averaging the resulting current density over the film thickness, yielding

$$\sigma^{\uparrow(\downarrow)}=\frac{ne^2}{2mv_F}\frac{1}{t}\int_0^t dz\frac{3}{4\pi}\int d^3\hat{v}\hat{v}_x^2\lambda_{\text{eff}}^{\uparrow(\downarrow)}(\hat{\mathbf{v}},z) . \quad (14)$$

Carrying out the integration over z, we obtain

$$\sigma^{\uparrow(\downarrow)}=\frac{ne^2}{2mv_F}\frac{3}{2\pi}\int_{v_z>0}d^3\hat{v}\hat{v}_x^2\lambda^{\uparrow(\downarrow)}(\vartheta)\left\{1-\frac{\lambda^{\uparrow(\downarrow)}(\vartheta)\hat{v}_z}{t}\left[1-\exp\left[\frac{-t}{\lambda^{\uparrow(\downarrow)}(\vartheta)\hat{v}_z}\right]\right]\right\} . \quad (15)$$

It is clear that our result is a straightforward extension of the Fuchs-Sondheimer theory.[13,14]

D. Cylindrical wires

In the case of a cylindrical wire with diameter $2R$ and the electric field applied along the wire (x) axis (Fig. 1), we use an equivalent approach as for the thin film. Again we assume diffusive boundary scattering, and similar boundary conditions as in Eq. (11) can be formulated. $\lambda_{\text{eff}}^{\uparrow(\downarrow)}(\hat{\mathbf{v}},\mathbf{r})$ is the mean distance traveled by an electron, with normalized velocity $\hat{\mathbf{v}}$, passing through a point $\mathbf{r}$ in the direction $\mathbf{r}_0-\mathbf{r}$, with $\mathbf{r}_0$ on the wire boundary. When assuming that electrons arriving at $\mathbf{r}_0$ scatter diffusely, it is easily shown that[19,20]

$$\lambda_{\text{eff}}^{\uparrow(\downarrow)}(\hat{\mathbf{v}},\mathbf{r})=\lambda^{\uparrow(\downarrow)}(\vartheta)\left[1-\exp\left[\frac{-|\mathbf{r}_0-\mathbf{r}|}{\lambda^{\uparrow(\downarrow)}(\vartheta)}\right]\right] . \quad (16)$$

In this expression $(\mathbf{r}_0-\mathbf{r})$ and $\hat{\mathbf{v}}$ have equal directions.

The conductivity per spin as a function of the angle between $\mathbf{M}$ and $\mathbf{E}$ now follows from integrating $g^{\uparrow(\downarrow)}(\hat{\mathbf{v}},r)$ combined with Eqs. (4) and (16) over velocity space and averaging the resulting current density over the cross-

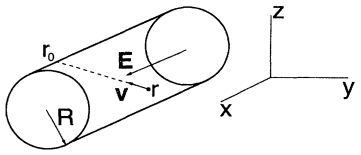

FIG. 1. Geometry of a cylindrical wire with radius R. The electric field vector **E** is directed along the wire axis.

sectional area $S=\pi R^2$ of the wire, yielding

$$\sigma^{\uparrow(\downarrow)}=\frac{ne^2}{2mv_F}\frac{1}{S}\int_S d^2r\frac{3}{4\pi}\int d^3\hat{v}\hat{v}_x^2\lambda_{\text{eff}}^{\uparrow(\downarrow)}(\hat{\mathbf{v}},r)\ . \tag{17}$$

E. Trilayers

We also study trilayer films of the type $F/NM/F$, where F and NM are ferromagnetic and nonmagnetic layers, respectively. Such trilayers show, in addition to the AMR effect, the spin valve or giant magnetoresistance (GMR) effect: the resistance depends on the angle between the magnetization vectors of the F layers. In experimental studies of such systems, the magnetization direction of one of the F layers is often fixed due to exchange interaction with a high coercivity ferromagnet, or with an antiferromagnetic layer ("exchange biasing"). Alternatively, it is possible to study systems for which both layers can rotate freely. In our theoretical study we concentrate on the exchange biased-type trilayer.[21] In order to calculate the combined AMR and GMR effect of trilayers with a ferromagnetic alloy, we have extended the semiclassical Boltzmann transport theory for the GMR effect, proposed by Camley and Barnás,[22] to include anisotropic spin-dependent scattering within the ferromagnetic layers. In the present model we neglect scattering at the F/NM interfaces. Refraction effects, related to potential steps at the interfaces, are not included, so m and v_F are constant throughout the system. A detailed theoretical study of the transport properties of magnetic multilayers, with or without these effects, has been done by Hood and Falicov[23] and Dieny,[24] respectively, however without taking the AMR effect into account.

Figure 2 shows the trilayer geometry with the magnetic layers A and C separated by the nonmagnetic layer B of thicknesses a, c, and b, respectively. For each individual layer solutions $g_{A,B,C}^{\uparrow(\downarrow)}(\mathbf{v},z)$ of the form of Eq. (12) are valid, which consequently should be matched according to the appropriate boundary conditions. For the case of purely diffusive scattering of electrons at the outer boundaries, complete transmission at the interfaces, and a change of the quantization axis at the NM/F interface at $z=a+b$, the boundary and interfacial conditions are[22]

$$g_A^{\uparrow(\downarrow)}(\hat{\mathbf{v}},0)=0,\quad \text{if } \hat{v}_z>0\ , \tag{18a}$$

$$\begin{aligned} &g_B^{\uparrow(\downarrow)}(\hat{\mathbf{v}},a)=g_A^{\uparrow(\downarrow)}(\hat{\mathbf{v}},a),\quad \text{if } \hat{v}_z>0\ ,\\ &g_B^{\uparrow(\downarrow)}(\hat{\mathbf{v}},a)=g_A^{\uparrow(\downarrow)}(\hat{\mathbf{v}},a),\quad \text{if } \hat{v}_z<0\ , \end{aligned} \tag{18b}$$

$$\begin{aligned} g_C^{\uparrow}(\hat{\mathbf{v}},a+b)&=T^{\uparrow\uparrow}g_B^{\uparrow}(\hat{\mathbf{v}},a+b)+T^{\downarrow\uparrow}g_B^{\downarrow}(\hat{\mathbf{v}},a+b)\ ,\\ &\qquad\text{if } \hat{v}_z>0\ ,\\ g_C^{\downarrow}(\hat{\mathbf{v}},a+b)&=T^{\downarrow\downarrow}g_B^{\downarrow}(\hat{\mathbf{v}},a+b)+T^{\uparrow\downarrow}g_B^{\uparrow}(\hat{\mathbf{v}},a+b)\ ,\\ &\qquad\text{if } \hat{v}_z>0\ , \end{aligned} \tag{18c}$$

$$\begin{aligned} g_B^{\uparrow}(\hat{\mathbf{v}},a+b)&=T^{\uparrow\uparrow}g_C^{\uparrow}(\hat{\mathbf{v}},a+b)+T^{\downarrow\uparrow}g_C^{\downarrow}(\hat{\mathbf{v}},a+b)\ ,\\ &\qquad\text{if } \hat{v}_z<0\ ,\\ g_B^{\downarrow}(\hat{\mathbf{v}},a+b)&=T^{\downarrow\downarrow}g_C^{\downarrow}(\hat{\mathbf{v}},a+b)+T^{\uparrow\downarrow}g_C^{\uparrow}(\hat{\mathbf{v}},a+b)\ ,\\ &\qquad\text{if } \hat{v}_z<0\ , \end{aligned} \tag{18d}$$

$$g_C^{\uparrow(\downarrow)}(\hat{\mathbf{v}},a+b+c)=0,\quad \text{if } \hat{v}_z<0\ . \tag{18e}$$

The transmission coefficients $T^{\uparrow\uparrow}$, $T^{\uparrow\downarrow}$, $T^{\downarrow\uparrow}$, and $T^{\downarrow\downarrow}$ determine the probability for a majority spin electron in one magnetic layer to continue as a majority spin or minority spin electron in the other magnetic layer, and are given by[22]

$$T^{\uparrow\uparrow}=T^{\downarrow\downarrow}=\cos^2\left[\frac{\psi}{2}\right]\ , \tag{19a}$$

$$T^{\uparrow\downarrow}=T^{\downarrow\uparrow}=\sin^2\left[\frac{\psi}{2}\right]\ , \tag{19b}$$

where ψ is the angle between both magnetizations. For example, in the case of an antiparallel arrangement of the magnetizations ($\psi=\pi$), $T^{\uparrow\uparrow}=T^{\downarrow\downarrow}=0$ and $T^{\uparrow\downarrow}=T^{\downarrow\uparrow}=1$. This means that a majority spin electron in one magnetic layer becomes a minority spin electron in the other magnetic layer, after traversing the nonmagnetic interlayer.

The conductivity of trilayer films, as a function of the orientation of the magnetization vectors, is calculated similar to the thin film case [Eq. (14)], but now averaging over the total thickness of the trilayer, in each region of the trilayer using the appropriate expressions for $g^{\uparrow(\downarrow)}(\hat{\mathbf{v}},z)$.

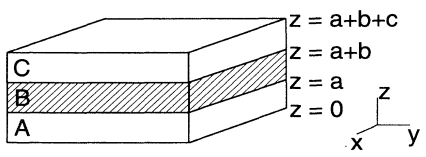

FIG. 2. Geometry of a magnetic trilayer consisting of magnetic layers A and C separated by nonmagnetic layer B.

III. RESULTS AND DISCUSSION

A. Parameter values

We apply the model, described in Sec. II, to NiFe thin films and cylindrical wires, and to NiFe/Cu/NiFe trilayers. For polycrystalline dilute bulk NiFe alloys at 4.2 K it was found by Dorleijn and co-workers[7,8] that

$$\left[\frac{\rho_{\parallel}-\rho_{\perp}}{\rho_{\parallel}}\right]^{\uparrow}=14\%, \quad \left[\frac{\rho_{\parallel}-\rho_{\perp}}{\rho_{\parallel}}\right]^{\downarrow}=-2.2\%\ , \qquad \left[\frac{\rho}{\rho^{\uparrow}}\right]_{\parallel}=\left[\frac{\sigma^{\uparrow}}{\sigma}\right]_{\parallel}=0.92\ , \tag{20}$$

where $\rho_{\parallel}$ is the resistivity for $\mathbf{M}\|\mathbf{E}$ and $\rho_{\perp}$ is the resistivity for $\mathbf{M}\perp\mathbf{E}$, $\sigma^{\uparrow}$ is the conductivity due to majority spin electrons, and $\sigma=\sigma^{\uparrow}+\sigma^{\downarrow}$ is the total conductivity. These data were determined by the analysis of the spin- and angular-resolved resistivities of ternary $Ni_{1-x}(Fe_yX_{1-y})_x$ alloys ($x\ll 1, 0<y<1, X$ is a metal).[7,8,25] From these data it follows that, at least in the dilute limit ($x\ll 1$), the conductivity of $Ni_{1-x}Fe_x$ alloys is mainly due to majority spin electrons and the AMR effect is governed by the anisotropic scattering of majority spin electrons.

It is apparent from Eq. (9) that Dorleijn's spin-resolved AMR data are not sufficient to determine both anisotropic scattering parameters, $a^{\uparrow(\downarrow)}$ and $b^{\uparrow(\downarrow)}$, separately. In one extremal case, when the $b^{\uparrow(\downarrow)}$ terms are set to zero, it follows that $a^{\uparrow}=0.327$, $a^{\downarrow}=-0.0556$, and $\lambda_0^{\uparrow}/\lambda_0^{\downarrow}=14.8$. On the other hand, when the $a^{\uparrow(\downarrow)}$ terms are set to zero it follows that $b^{\uparrow}=0.395$, $b^{\downarrow}=-0.0645$, and $\lambda_0^{\uparrow}/\lambda_0^{\downarrow}=14.2$. As a result of our calculations, we find that the AMR ratio for films, wires, and multilayers is only very weakly dependent on the ratio of the $\cos^2\vartheta$ to the $\cos^4\vartheta$ contribution to the angular dependence of the mean free path [Eq. (4)]. An explicit example will be given for the case of a thin film. Our other examples are based on the first parameter set, neglecting the $\cos^4\vartheta$ term. We are confident that from these examples, in spite of this restriction, a very good picture if offered on dimensionality effects in the AMR effect. For future reference, in Table I values of $a^{\uparrow}$, $a^{\downarrow}$, $\lambda_0^{\uparrow}/\lambda_0^{\downarrow}$, and $\Delta\rho/\rho$ are listed for a number of dilute nickel alloys, based on the experimental data of Dorleijn, and again assuming that $b^{\uparrow(\downarrow)}=0$. These data are independent of the impurity concentration. It is interesting to note that the impurity scattering (parametrized by $a^{\uparrow(\downarrow)}$), which gives rise to the AMR effect, is much more anisotropic than the resistance itself.

TABLE I. Anisotropic scattering parameters, spin dependence of the scattering, and AMR ratio for bulk dilute nickel alloys, based on spin-resolved resistivity data of Dorleijn and coworkers (Refs. 7 and 8) (4.2 K).

Solute element	$a^{\uparrow}$	$a^{\downarrow}$	$\lambda_0^{\uparrow}/\lambda_0^{\downarrow}$	$\Delta\rho/\rho_{\parallel}$ (%)
Co	0.336	−0.0378	17.0	13.5
Fe	0.327	−0.0556	14.8	12.9
Mn	0.229	−0.0839	7.45	7.8
Au	0.195	−0.0556	7.19	7.5
Cu	0.231	−0.0531	3.41	6.8
Zn	0.188	−0.0736	2.75	4.6
Al	0.176	−0.0582	1.97	3.8
Sn	0.153	−0.0684	1.87	2.9
Si	0.150	−0.0813	1.47	2.1
Ti	0.103	−0.0813	1.07	0.55
V	0.190	−0.0787	0.531	0.15
Re	0.157	−0.0607	0.361	−0.50
Rh	0.188	−0.0582	0.348	0.05
Ir	−0.0633	−0.0352	0.231	−1.48
Pt	0.141	−0.0201	0.259	0.40
Cr	0.141	−0.0429	0.230	−0.35
Ru	0.183	−0.0277	0.080	−0.60

In the numerical calculations we use for NiFe the values $\lambda_0^{\uparrow}=120$ Å and $\lambda_0^{\downarrow}=8$ Å, their ratio complying with the value given above, and the $a^{\uparrow(\downarrow)}$ given above. We note that the actual choice of $\lambda_0^{\uparrow}$ and $\lambda_0^{\downarrow}$, given a certain ratio between these quantities, only affects the thickness scale below which dimensionality effects become sizable, and not the general behavior. In the dilute limit, with impurity scattering only, thickness scales are inversely proportional to the impurity concentration. The present values of $\lambda_0^{\uparrow}$ and $\lambda_0^{\downarrow}$ are expected to correspond to impurity concentrations of about 20% Fe. This follows from an order-of-magnitude calculation using the experimental residual resistance of majority spin electrons in NiFe systems ($\rho^{\uparrow}=0.44\times10^{-8}$ Ωm/at. %),[7,8] and using the simple expression $\rho^{\uparrow}=mv_F/n^{\uparrow}e^2\lambda^{\uparrow}$ with values of v_F and $n^{\uparrow}$ as appropriate for Cu, m being the free-electron mass. Using similar values of $\lambda^{\uparrow}$ and $\lambda^{\downarrow}$ for bulk scattering in permalloy ($Ni_{80}Fe_{20}$), Dieny[26] was able to quantitatively analyze the GMR effect of $Ni_{80}Fe_{20}/Cu/Ni_{80}Fe_{20}/Fe_{50}Mn_{50}$ "spin valve" multilayers. However, we note that in this study no intrinsic anisotropic scattering was taken into account. We will return to this issue later. For the Cu layer we assume isotropic spin-independent scattering, with $\lambda_0^{\uparrow}=\lambda_0^{\downarrow}=135$ Å, inspired again by the analysis of "spin valve" multilayers.[26] We note that this value of λ(Cu) is much smaller than the intrinsic mean free path of a pure copper crystal at 4.2 K, and should therefore be regarded as the result of scattering due to growing imperfections and grain boundaries, which are present in thin films.

B. Numerical results

In Fig. 3 the calculated AMR ratio for a NiFe film is given, which shows a monotonic decrease with decreasing

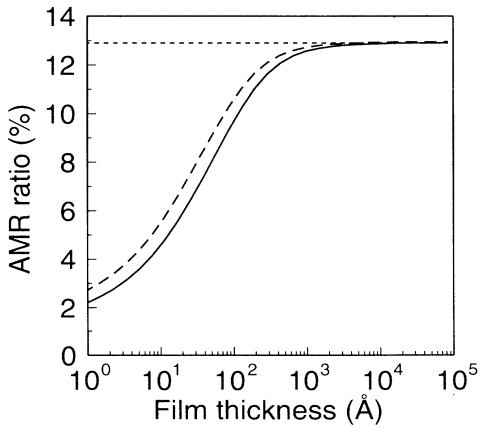

FIG. 3. AMR ratio as a function of the film thickness with the magnetization rotating in the film plane. For the solid line the $a^{\uparrow(\downarrow)}$ parameters are used ($b^{\uparrow(\downarrow)}=0$), for the dashed line the $b^{\uparrow(\downarrow)}$ parameters ($a^{\uparrow(\downarrow)}=0$). The small dashed line represents the bulk value.

film thickness, deviating significantly from the bulk value for thicknesses below a few hundreds of Å. The solid curve gives the result based on the set of $a^{\uparrow(\downarrow)}$ parameters discussed above (taking $b^{\uparrow(\downarrow)}=0$), and the dashed curve gives the result based on the set of $b^{\uparrow(\downarrow)}$ parameters (taking $a^{\uparrow(\downarrow)}=0$). It can be seen that the predictions, based on these rather extremal cases, are very similar. As discussed above, this has motivated us to neglect in further discussions the possible presence of a $\cos^4\vartheta$ term in the expression of the anisotropic mean free path [Eq. (4)].

The calculated normalized resistivity of a thin film of 200 Å NiFe as a function of the angle Θ between **M** and **E** is shown in Fig. 4. The resistivity was calculated with the magnetization rotating in the film (xy) plane (solid line) and rotating in the xz plane (dashed line), perpendicular to the film plane. For both cases the angular variation is found to be described approximately, but not precisely, by a $\cos^2\Theta$ function. The amplitude of the effect is larger in the out-of-plane case, as compared to the in-plane case. Figures 5(a) and 5(b) show the AMR ratio as a function of film thickness, the out-of-plane AMR ratio being even slightly larger than the bulk value for thicknesses above 200 Å. For the case of a wire Fig. 5(c) shows a monotonic decrease of the AMR ratio with decreasing wire diameter $2R$, which is even steeper than for the in-plane AMR effect in a film.

As the basis of a more detailed discussion on the origin of these results, the variation with thickness of the normalized resistivity change $\Delta\rho/\Delta\rho_\infty=(\rho_\parallel-\rho_\perp)/(\rho_\parallel-\rho_\perp)_\infty$, and of the normalized resistivity for $\mathbf{M}\|\mathbf{E}$, $\rho_\parallel/\rho_{\parallel,\infty}$ are given in Figs. 6 and 7, respectively. $\Delta\rho_\infty$ and $\rho_{\parallel,\infty}$ are the bulk values. Figure 6 shows that the resistivity change $\Delta\rho$ for the thin-film case is nearly independent of the film thickness for films thicker than about 100 Å [in-plane case, (a)] or about 500 Å [out-of-plane case, (b)]. For thinner films $\Delta\rho/\Delta\rho_\infty$ increases. The effects shown in Figs. 4–7 can be understood when considering only majority spin electrons, as (i) they carry the major part of the current, and (ii) dimensionality effects due to minority spin electrons are very small because of their small mean

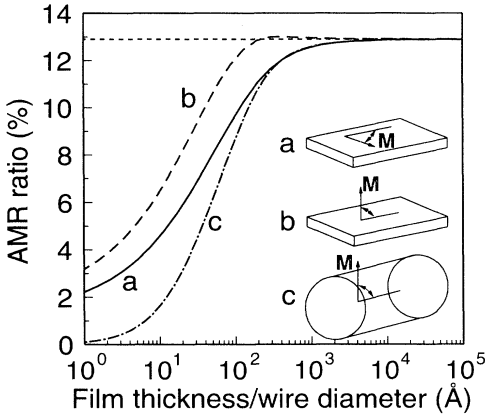

FIG. 5. AMR ratio as a function of film thickness or wire diameter (a) for a thin film with the magnetization rotating in the film plane, (b) for a thin film with the magnetization rotating out of the film plane, and (c) for a cylindrical wire. The small dashed line represents the bulk value.

free path. It follows from Eq. (4), with the values for $a^\uparrow$ and $a^\downarrow$ given above, that majority spin electrons with a large velocity component collinear to the magnetization direction experience the strongest scattering. Thus, as is illustrated in Fig. 4, the highest resistivity is found when the magnetization is collinear to the electric field and the resistivity drops when the magnetization vector is oriented perpendicular to the electric field. When the film thickness decreases, diffusive scattering at the film boundaries leads to an increase in resistivity, as shown in Fig. 7. Curves (a) and (b) in Fig. 6 show that this increase depends on the orientation of the magnetization. This can be explained by the fact that the contribution to the current of electrons with a velocity vector that deviates from **E** is larger in the case that $\mathbf{M}\|\mathbf{E}$ than in the case that $\mathbf{M}\perp\mathbf{E}$, so that diffusive boundary scattering influences $\rho_\parallel$ more than $\rho_\perp$. However, the stronger increase in resistivity with decreasing film thickness leads to a decreasing AMR ratio as the net effect.

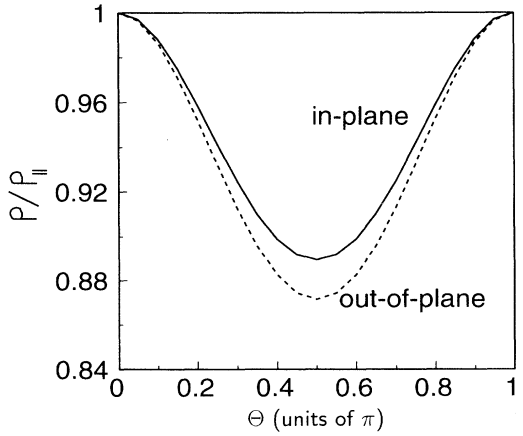

FIG. 4. Calculated normalized resistivity as a function of the angle Θ between **M** and **E** of a 200 Å NiFe thin film, with the magnetization rotating in the film (xy) plane (solid), and rotating in the xy plane (dashed), perpendicular to the film plane.

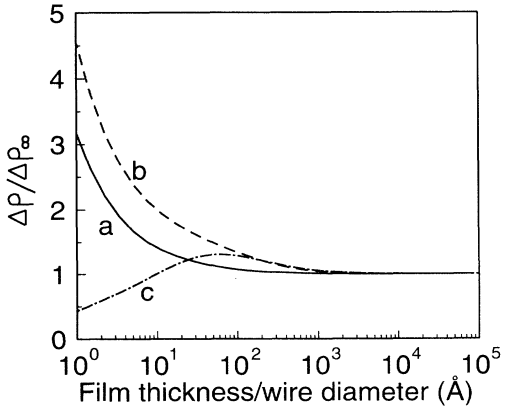

FIG. 6. Normalized resistivity change $\Delta\rho/\Delta\rho_\infty$ as a function of film thickness or wire diameter (a) for a thin film with the magnetization rotating in the film plane, (b) for a thin film with the magnetization rotating out of the film plane, and (c) for a cylindrical wire. $\Delta\rho_\infty$ is the bulk resistivity change.

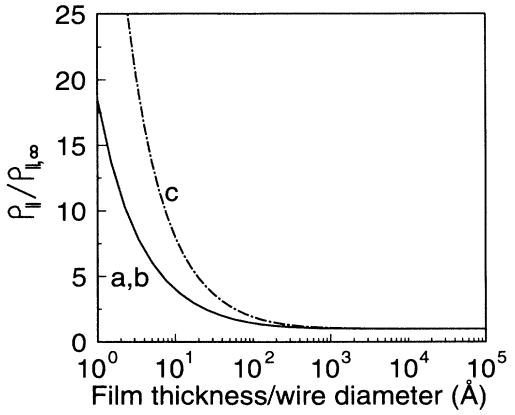

FIG. 7. Normalized resisitivity as a function of film thickness (solid) or wire diameter (chain dashed), in the case of $\mathbf{M}\|\mathbf{E}$. ρ_∞ is the bulk resistivity.

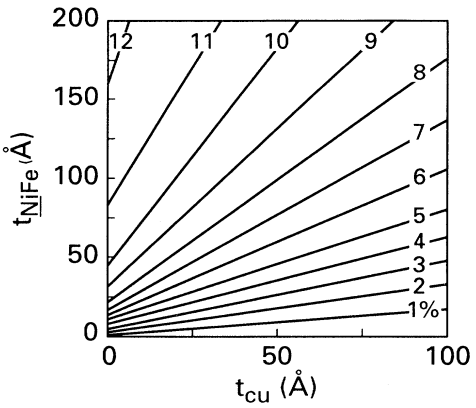

FIG. 8. AMR ratio (%) of a NiFe/Cu/NiFe trilayer film, as a function of the NiFe and Cu layer thickness, with parallel magnetizations.

Due to the fact that $\rho_\perp$ ($\mathbf{M}$ in plane) increases more strongly with decreasing film thickness than $\rho_\perp$ ($\mathbf{M}$ out of plane), the AMR ratio for thin films is smaller when the magnetization rotates in the film plane than when the magnetization rotates from in plane ($\mathbf{M}\|\mathbf{E}$) to perpendicular to the film plane ($\mathbf{M}\perp\mathbf{E}$). In the out-of-plane case the influence of diffusive scattering at the film boundaries is reduced because the anisotropic scattering limits the mean free path of electrons with a large velocity component perpendicular to the film plane.

In order to understand the results for cylindrical wires, we are forced to reconsider the point of view that the majority spin electrons determine the AMR in all cases. Figure 6 [curve (c)] shows that $\Delta\rho$ ultimately decreases for small wire diameters, in contrast to the case of thin films. In a cylindrical wire, the outer boundaries have a strong influence on the resistivity [curve (c) in Fig. 7]. The contribution to the current of majority spin electrons, that have a relatively large mean free path, depends more strongly on the wire diameter than the contribution of the minority spin electrons. For a very small wire diameter the majority spin electrons experience a strong diffusive scattering at the outer boundaries, leading to a relatively large contribution of the minority spin electrons to the total current and to the AMR. As the contribution to the AMR ratio due to minority spin electrons is negative in NiFe [see Eq. (20) or, equivalently, $a^{\downarrow}$ is negative], the total resistivity change $\Delta\rho$ decreases with decreasing wire diameter.

The results of the calculations on NiFe/Cu/NiFe trilayers are summarized in Figs. 8 and 9.[18] The magnetization of one of the NiFe layers is fixed, the magnetization of the other NiFe layer can be freely rotated. Figure 8 shows the calculated values of the AMR ratio as a function of the Cu-layer thickness t_{Cu} and the NiFe-layer thickness t_{NiFe}, defined as

$$\mathrm{AMR}(P)\equiv\frac{\rho(P,\mathbf{M}\|\mathbf{E})-\rho(P,\mathbf{M}\perp\mathbf{E})}{\rho(P,\mathbf{M}\|\mathbf{E})}\ , \tag{21}$$

the magnetizations being mutually parallel (P). In Fig. 8 it can clearly be noticed that shunting by the Cu interlayer gives a considerable reduction of the AMR ratio. For $t_{NiFe}=200$ Å and $t_{Cu}\approx 0$ Å the bulk value of 12.9% for the AMR ratio is almost reached. Figure 9 shows the calculated GMR ratio as a function of t_{Cu} and t_{NiFe}, defined as

$$\mathrm{GMR}(\mathbf{M}\|\mathbf{E})\equiv\frac{\rho(AP,\mathbf{M}\|\mathbf{E})-\rho(P,\mathbf{M}\|\mathbf{E})}{\rho(P,\mathbf{M}\|\mathbf{E})}\ . \tag{22}$$

The magnetizations, in a parallel (P) or antiparallel (AP) arrangement, are collinear to the electric field $\mathbf{E}$. From Fig. 9 we can see that the maximum in GMR ratio is achieved at very low thickness, for $t_{Cu}\to 0$ Å and $t_{NiFe}=20$ Å. For a finite t_{Cu} the GMR ratio is reduced because of shunting and a decreasing probability for electrons to cross the Cu interlayer without scattering. For large t_{NiFe} it is also shunting that causes the reduction in GMR ratio. For very small t_{NiFe} diffusive scattering of the majority spin electrons at the outer boundaries reduces the difference in the scattering of spin-up and spin-down electrons and increases the resistivity. Therefore the GMR ratio decreases. The dashed line in Fig. 9 marks the t_{NiFe} with the highest GMR, as a function of t_{Cu}. It shows that, in order to maximize the GMR, t_{NiFe} must be enlarged with increasing t_{Cu}, thereby preventing the current from running mainly through the Cu layer.

In Fig. 10 the quantity Δ_{GMR}, which is defined as

$$\Delta_{\mathrm{GMR}}=\frac{[\rho(AP,\mathbf{M}\|\mathbf{E})-\rho(P,\mathbf{M}\|\mathbf{E})]-[\rho(AP,\mathbf{M}\perp\mathbf{E})-\rho(P,\mathbf{M}\perp\mathbf{E})]}{\rho(P,\mathbf{M}\|\mathbf{E})} \tag{23}$$

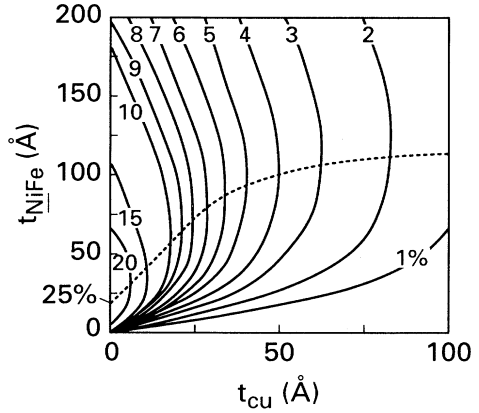

FIG. 9. GMR ratio (%) of a NiFe/Cu/NiFe trilayer film, as a function of the NiFe and Cu layer thickness, with the magnetizations parallel to the direction of the electric field. The dashed line connects points, for each Cu thickness, of optimal NiFe thickness.

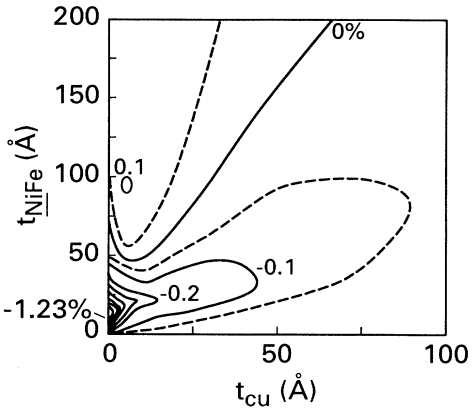

FIG. 10. Δ_{GMR}, that represents the influence of anisotropic scattering on the GMR, as a function of the NiFe and Cu layer thickness.

is plotted as a function of t_{NiFe} and t_{Cu}. Δ_{GMR} represents the influence of anisotropic scattering on the GMR ratio. Comparison of Figs. 9 and 10 shows that $\Delta_{GMR}/GMR(\mathbf{M}\|\mathbf{E})$ can reach at least 10 to 20% in areas where GMR is very small and Δ_{GMR} is large enough, e.g., for $t_{Cu}\approx 10$ Å and t_{NiFe} very small. Trends in Fig. 10 can be understood when taking the following three points into account. (i) According to Eq. (4) the average value of $\lambda^{\uparrow}$ (NiFe) for electrons is smallest in the case of $\mathbf{M}\|\mathbf{E}$. The spin dependence of the scattering is therefore smaller than in the case of $\mathbf{M}\perp\mathbf{E}$. This effect gives a negative contribution to Δ_{GMR} and becomes more important for decreasing NiFe layer thickness. In the case of thin NiFe layers most of the current is carried by electrons with a velocity vector close the current direction, due to the diffusive scattering at the boundaries. (ii) As mentioned before in the case of $\mathbf{M}\|\mathbf{E}$, the enhanced scattering of spin-up electrons parallel to the current direction results in a relatively larger contribution to the current from electrons with a large velocity component perpendicular to the plane of the layers. This is most important for large NiFe thickness and results in a positive contribution to Δ_{GMR}. In this case diffusive scattering at the boundaries does not severely limit the contribution to the current of electrons with a large perpendicular velocity component. (iii) When the GMR decreases, the absolute value of Δ_{GMR} decreases.

The dependence of the AMR ratio on the mutual alignment of the magnetic layers follows from the quantity Δ_{AMR}, which is defined as

$$\Delta_{AMR}=\frac{[\rho(P,\mathbf{M}\|\mathbf{E})-\rho(P,\mathbf{M}\perp\mathbf{E})]-[\rho(AP,\mathbf{M}\|\mathbf{E})-\rho(AP,\mathbf{M}\perp\mathbf{E})]}{\rho(P,\mathbf{M}\|\mathbf{E})}\ . \tag{24}$$

From comparison of Eqs. (23) and (24) it follows that $\Delta_{AMR}=-\Delta_{GMR}$. The conditions where the GMR ratio is relatively sensitive to the current direction therefore precisely coincide with the conditions where the AMR ratio is relatively sensitive to the mutual alignment of the F layers. For the usual layer thicknesses in spin-valve structures[21] these cross effects are very small.

Our predictions of the AMR effect in thin films can easily be checked by performing resistivity measurements at helium temperature on a ferromagnetic alloy for varying film thickness, by rotating the sample in a saturating field. In-plane measurements of the AMR effect have already been carried out by McGuire and Potter[6] in permalloy thin films. The results of these measurements, although they were carried out at room temperature, roughly support our predictions. The out-of-plane measurements will require fairly high fields, because of demagnetization effects. According to our predictions the cylindrical wire case seems to be very suitable for determining the minority spin contribution to the AMR effect. However, the AMR effect in the wire case will be very complicated to check experimentally, mainly because of the difficulties of preparing cylindrical samples with a diameter small enough to measure size effects.

In polycrystalline samples, apart from intrinsically anisotropic scattering processes also extrinsically anisotropic scattering processes can play an important role, as was shown by Dieny,[26] who was able to quantitatively analyze the GMR effect in $Ni_{80}Fe_{20}/Cu/Ni_{80}Fe_{20}/Fe_{50}Mn_{50}$ multilayers by taking grain boundary scattering into account. In a forthcoming paper we will present the results of an analysis of the resistivity of ferromagnetic thin films and $M/Cu/M/Fe_{50}Mn_{50}$ "spin-valve" multilayers (M is a ferromagnetic metal) by taking intrinsically anisotropic scattering as well as scattering at grain boundaries into account.

IV. CONCLUSIONS

We have carried out model calculations of the resistivity by solving the Boltzmann transport equation in linear response for a free-electron gas in the relaxation-time approximation. Our most crucial additional assumption, in order to treat the anisotropic magnetoresistance effect, is

that the electron mean free path depends on the angle between the electron velocity vector and the magnetization vector.

We have applied this model to bulk ferromagnetic systems, thin films, cylindrical wires, and trilayers of the type $F/NM/F$, where F and NM are ferromagnetic and nonmagnetic layers, respectively. Numerical examples have been given for dilute NiFe alloys. For a thin film, the AMR ratio in the case where **M** rotates out of the film plane is predicted to be considerably higher than in the case where **M** rotates in the film plane. Although the AMR ratio decreases with decreasing film thickness, the resistivity change $\Delta\rho$ increases. This is due to the fact that influence of diffusive scattering of electrons at the film boundaries depends on the magnetization orientation. The AMR ratio for a cylindrical wire decreases rapidly if the wire diameter becomes smaller than the relevant mean free path, and even $\Delta\rho$ decreases for sufficiently low diameters. This is due to the contribution of the minority spin electrons, which cannot be neglected when the diameter becomes much smaller than the mean free path of the majority spin electrons.

Our calculations of $F/NM/F$ trilayers have revealed to what extent AMR and GMR can be treated as two superimposed effects. In a limit range of F-layer and NM-layer thickness, the difference in GMR ratio in the case of $\mathbf{M}\|\mathbf{E}$ and $\mathbf{M}\perp\mathbf{E}$ can be larger than 10%. However, treating the combined effect of AMR and GMR in terms of a simple summation of both phenomena is, in almost the entire thickness region studied, precise within a few tenths of a percent.

ACKNOWLEDGMENT

This research is part of the European Community ESPRIT3 Basic Research Project, "Study of Magnetic Multilayers for Magnetoresistive Sensors" (SmMmS), and was supported by the Technology Foundation (STW).

[1]W. Thomson, Proc. R. Soc. **8**, 546 (1857).
[2]J. Smit, Physica **16**, 612 (1951).
[3]L. Berger, Physica **30**, 1141 (1964).
[4]R. I. Potter, Phys. Rev. B **10**, 4626 (1974).
[5]H. C. van Elst, Physica **25**, 708 (1959).
[6]T. R. McGuire and R. I. Potter, IEEE Trans. **MAG-11**, 1018 (1975).
[7]J. W. F. Dorleijn and A. R. Miedema, J. Phys. F **5**, 1543 (1975).
[8]J. W. F. Dorleijn, Philips Res. Rep. **31**, 287 (1976).
[9]O. Jaoul, I. A. Campbell, and J. Fert, J. Magn. Magn. Mater. **5**, 23 (1977).
[10]F. W. Gorter, J. A. L. Potgiesser, and D. L. A. Tjaden, IEEE Trans. **MAG-10**, 899 (1974).
[11]D. A. Thompson, L. T. Romankiw, and A. F. Mayadas, IEEE Trans. **MAG-11**, 1039 (1975).
[12]A. F. Mayadas, J. F. Janak, and A. Gangulee, J. Appl. Phys. **45**, 2780 (1974).
[13]K. Fuchs, Proc. Cambridge Philos. Soc. **34**, 100 (1938).
[14]E. H. Sondheimer, Philos. Mag. Suppl. **1**, No. 1, p. 1 (1952).
[15]N. F. Mott, Proc. R. Soc. **153**, 699 (1936).
[16]M. N. Baibich, J. Broto, A. Fert, F. Nguyen Van Dau, F. Petroff, P. Etienne, G. Creuzet, A. Friederich, and J. Chazelas, Phys. Rev. Lett. **61**, 2472 (1988).
[17]G. Binasch, P. Grünberg, F. Saurenbach, and W. Zinn, Phys. Rev. B **39**, 4828 (1989).
[18]Th. G. S. M. Rijks, R. Coehoorn, and W. J. M. de Jonge, in *Magnetic Ultrathin Films,* edited by B. T. Jonker, MRS Symposia Proceedings No. 313 (Materials Research Society, Pittsburgh, 1993), p. 283.
[19]R. G. Chambers, Proc. R. Soc. A **202**, 378 (1950).
[20]R. B. Dingle, Proc. R. Soc. A **201**, 545 (1950).
[21]B. Dieny, V. S. Speriosu, S. Metin, S. S. P. Parkin, B. A. Gurney, P. Baumgart, and D. R. Wilhoit, J. Appl. Phys. **69**, 4774 (1991).
[22]R. E. Camley and J. Barnás, Phys. Rev. Lett. **63**, 664 (1989).
[23]R. Q. Hood and L. M. Falicov, Phys. Rev. B **46**, 8287 (1992).
[24]B. Dieny, J. Phys. Condens. Matter **4**, 8009 (1992).
[25]A. Fert and I. A. Campbell, J. Phys. F **6**, 849 (1976).
[26]B. Dieny, Europhys. Lett. **17**, 261 (1992).